SINGLE SPIKE OPERATION FOR THE GENERATION OF SUB-FS PULSES IN THE NEW LIGHT SOURCE

R. Bartolini[1,2,#], I.P.S. Martin[1,2], J.H. Han[1] and J.H. Rowland[1]

[1]Diamond Light Source Ltd, Oxfordshire, OX11 0QX, UK.
[2]John Adams Institute, University of Oxford, OX1 3RH, UK,

Abstract

We discuss the possible operation of the UK New Light Source in the single spike regime with photon energies up to 1 keV. The optimisation process of the beam dynamics in the single spike regime is outlined and we present the results of full start-to-end simulations to show that sub-fs pulses can be obtained with interesting power levels. The analysis of the jitter of the SASE output characteristic is also reported.

INTRODUCTION

The New Light Source (NLS) Project in the UK [1] will be based on a combination of advanced conventional laser and free electron laser (FEL) sources. The latter will provide radiation with the following characteristics

- photon energy range from 50 eV to 1 keV
- high brightness (>10^{11} photons per pulse at 1 keV)
- repetition rate > 1 kHz
- variable polarisation
- short pulses of 20 fs FWHM or less
- temporal and transverse coherence

The upgrade path of the NLS project foresees the generation of ultrashort radiation pulses which will enable a variety of pump-probe experiments to be carried out on femtosecond (fs) time scales or below.

One of the most straightforward schemes for generating fs pulses is based on an idea originally proposed by Bonifacio and coworkers [2]. In his seminal paper Bonifacio showed that if the electron r.m.s. bunch length is shorter than the FEL cooperation length it will generate a single SASE radiation spike which is both temporally and transversely coherent. This idea has been recently reconsidered for the case of an ultra low electron bunch charge [3]. Numerical investigations have shown that single spike operation can be reached with bunch charges of the order of few pC [3,4]. These conditions allow an efficient compression since collective effects such as transverse space charge in the injector and coherent synchrotron radiation (CSR), longitudinal space charge (LSC) and wakefield effects are considerably reduced. The weaker collective effects allow an extremely high beam quality to be achieved at the RF photocathode gun and compression factors in the linac to be an order of magnitude larger than the ones typically applied for standard SASE operation. Such bunches would provide a brightness (measured as $I/\varepsilon_x\varepsilon_y$) which is significantly greater than in standard FEL SASE operation, with correspondingly shorter gain lengths.

Such an operating mode is very appealing for the NLS project since it has the potential to generate sub-fs coherent radiation pulses without the introduction of new hardware, requiring only a modest retuning of the linac working point. This operating mode is not without its drawbacks however, with accurate synchronisation and the operation of diagnostic equipment at such low charges of particular concern. Indeed the use of such ultrashort radiation pulses in pump-probe experiments imposes tight tolerances on the timing jitter of the electron bunch. The intrinsic variability of the SASE power level in the single spike operation also needs to be considered.

In this paper we describe the optimisation of the working point of the NLS linac for single spike operation. We also analyse the jitter in power levels expected for the single spike operation from the electron bunch and compare them to the intrinsic jitter coming from different shot noise seeds in the SASE simulations.

NLS LAYOUT FOR SINGLE SPIKE OPERATION

The layout of the NLS linac is described in [5] and we refer the reader to this paper for the details and the rationale for the choice of this machine layout. The linac operation for single spike emission was optimised with the specific aim of proving that it can be achieved without requiring any changes to the hardware configuration.

The electron gun parameters were optimised for 1 pC and 10 pC bunch charges [6]. The main parameters at the end of the injector are summarised in Tab. 1, and phase space plots for the 10 pC case are shown in Fig. 1. Further optimisation and simulation of intermediate bunch charges are planned for the near future. In this paper, linac operation with an intermediate charge value of 2 pC has been carried out using the 10 pC beam values and scaling the charge. This provides a conservative estimate of the achievable beam qualities.

Table 1: Electron bunch parameter at the end of the injector for 1 pC and 10 pC operation.

Bunch charge (pC)	1	10
Energy (MeV)	108.9	109.0
R.m.s. bunch length (ps)	2.5	9
Peak current (A)	0.5	1.25
R.m.s. norm. emittance (μm)	0.052	0.071
Slice norm. emittance (μm)	0.048	0.067
Slice energy spread	$2.3\cdot10^{-6}$	$6\cdot10^{-6}$

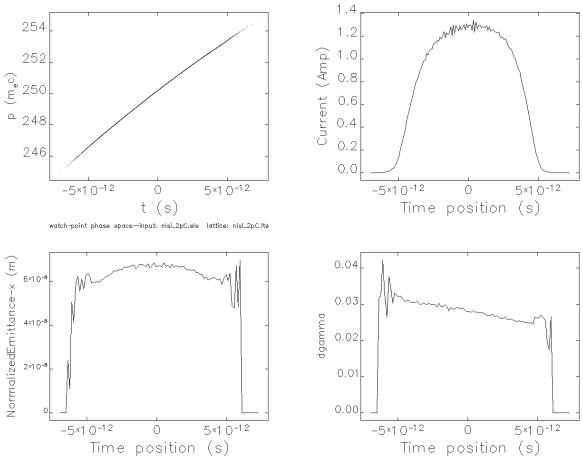

Figure 1: Longitudinal phase space of the electron bunch at the end of the injector for 10 pC operation.

The beam dynamics in the linac are optimised so as to produce the maximum possible compression before the FEL. This aggressive compression generates a bunch with a peak current high enough to reintroduce significant CSR effects when passing through the spreader section, as can be seen in Fig. 2. The present optimisation of the spreader section shows large energy loss for the electrons in the central spike, requiring a correction of the T_{566} term in the transfer matrix in order to prevent a broadening of the electron bunch length due to the internal energy variation. The benefits of this higher order correction are shown in Fig. 3, in which the longitudinal phase space and current distributions are shown with and without sextupoles powered. The sextupole scheme also applies local chromaticity correction to limit the CSR-driven blow-up in the horizontal emittance. This has been only partially successful, with the maximum tolerable bunch charge still limited to 2 pC. Under these conditions it is possible to generate an electron bunch with 2 kA peak current and a FWHM of 0.6 fs. The normalised emittance in the electron pulse is still below 0.3 μm as shown in Fig. 4. Optimisation of the spreader section is ongoing.

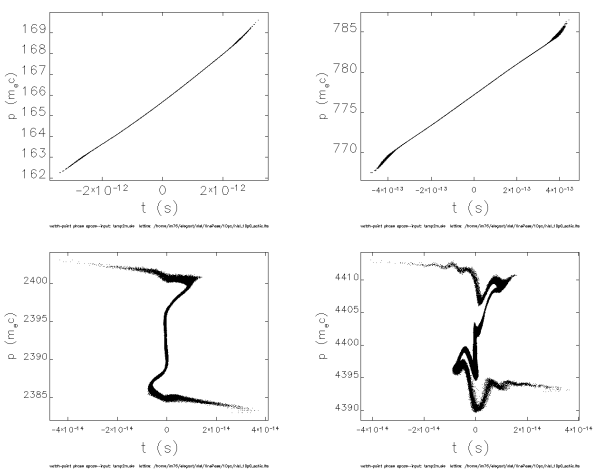

Figure 2: Longitudinal phase space at the end of the bunch compressors: BC1 (top left), BC2 (top right), BC3 (bottom left) and at the end of the spreader (bottom right).

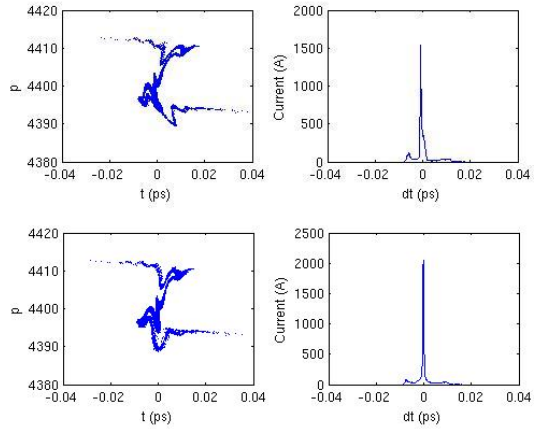

Figure 3: Longitudinal phase space and current distribution plots at the FEL with (bottom) and without (top) sextupole correction in the spreader section.

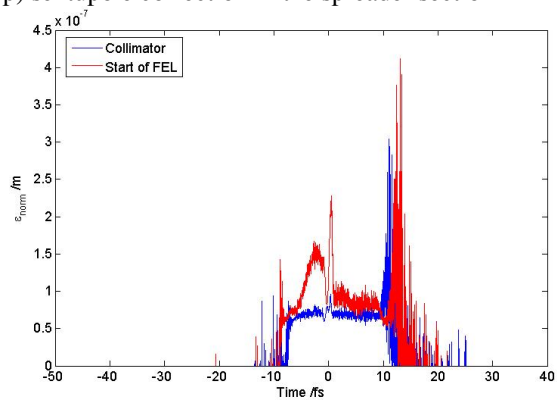

Figure 4: Emittance of the electron bunch at the end of the collimator and at the beginning of the FEL. Notice that most of the current is in the central spike located near t=0.

JITTER STUDIES

Variation in power supplies (PS), electron gun (G), RF cavity phases (P) and cavity voltages (V) leads to unavoidable jitter in the electron bunch at the FEL. The effects of these error sources on the arrival time and beam quality have been estimated using the ASTRA [7] and ELEGANT [8] tracking codes. The tolerance values used in the simulations are summarised in Tab. 2.

Table 2: Tolerances used in the jitter simulations

RF gun phase	0.1 deg
RF gun voltage	10^{-3}
Gun solenoid PS	$5{\cdot}10^{-5}$
Main RF cavity phase	0.01 deg
Main RF cavity voltage	10^{-4}
Bunch compressor PS	$1{\cdot}10^{-5}$

In the simulations, the RF distribution was split in eight power sources per module (one per TESLA cavity). The current distributions for 100 error seeds are shown in Fig. 5, and show the variation in arrival time, peak current and bunch length. Pump-probe experiments will suffer from this level of jitter unless tighter tolerances can be met for the RF system.

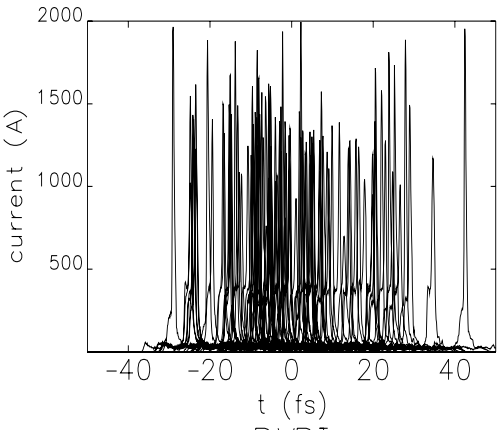

Figure 5: Variation in the bunch current distribution for 100 error seeds.

A summary of the jitter in arrival time, peak current and electron bunch FWHM is given in Tab. 3, in which the contributions due to the different error sources have been separately studied. The most significant source of timing jitter is the combination of the electron gun plus first accelerating module comprising the injector. The most significant source of a reduction in peak current and broadening of the electron bunch length is produced by phase and voltage errors in the electron gun; however, this effect is reduced when combined with all sources of error. Histograms of the peak current and electron bunch FWHM for the 100 seeds are shown in Figs. 6 and 7.

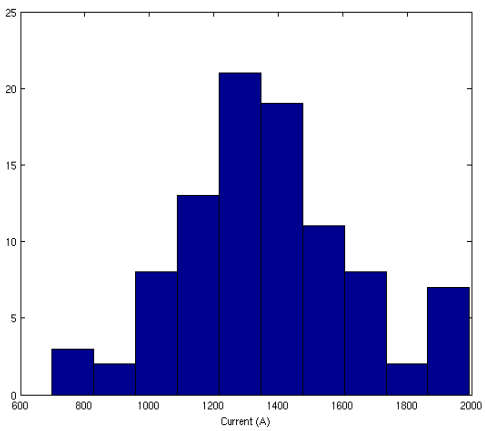

Figure 6: Histogram of the peak current over 100 seeds.

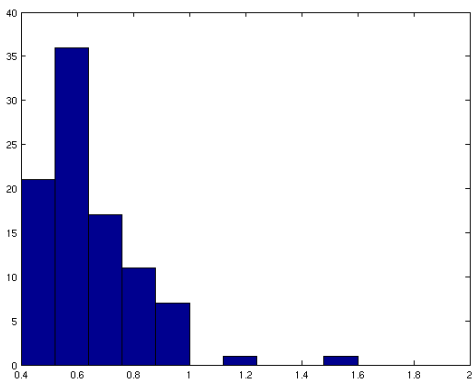

Figure 7: Histogram of the bunch length over 100 seeds.

Table 3: Electron bunch jitter for single spike operation

	Arrival time (fs)	Peak Current (A)	Bunch Length FWHM (fs)
RF gun (P and V)	7	1009 ± 139	0.92 ± 0.21
Injector (Gun + 1st module)	14	1386 ± 223	0.62 ± 0.11
Chicanes (PS)	1	1350 ± 91	0.59 ± 0.06
Linac (P + V + PS)	6	1329 ± 152	0.63 ± 0.10
Linac + Inj. (P + V + PS)	15	1368 ± 267	0.66 ± 0.17

FEL DYNAMICS

Even in the presence of a perfectly stable electron beam, the SASE FEL emission generated by the shot noise in the electron bunch will be subject to fluctuations. This effect was estimated in the single spike regime by performing 100 time dependent simulations with GENESIS varying the initial shot noise input seed. These simulations do not include the jitter on the electron bunch described earlier.

The arrival time of the FEL pulse has an intrinsic jitter of less than 1 fs and is therefore negligible with respect to that due to the gun and linac. Shown in Figs. 8 and 9 are the temporal and spectral profiles for the radiation pulses produced by the first 7 shot noise seeds for the ideal electron bunch at 27.6 m into the undulator train (after 6 undulator modules). The corresponding curves of power as a function of distance along the undulator train for each seed are given in Fig. 10. As can be seen there is a large intrinsic variability in the power levels and gain lengths due to the random nature of the SASE process.

The variation in the main radiation characteristics are summarized in Tab. 4. It is clear that, even after neglecting the variability in electron bunch quality demonstrated earlier there is still a significant variation in radiation pulse duration and spectral bandwidth in addition to the power variability. A histogram of the peak power levels over the 100 seeds is given in Fig. 11, the distribution of the pulse length is shown in Fig. 12 and the time-bandwidth product is given in Fig. 13.

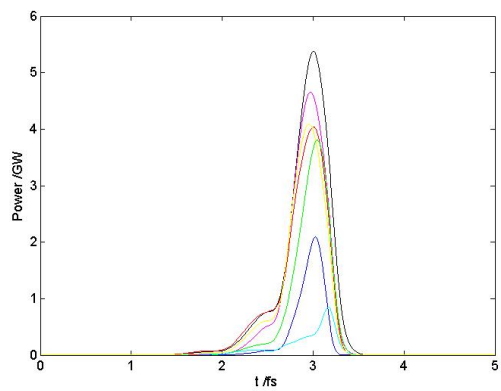

Fig. 8: Example of the temporal profile for 7 pulses with different initial shot noise seeds.

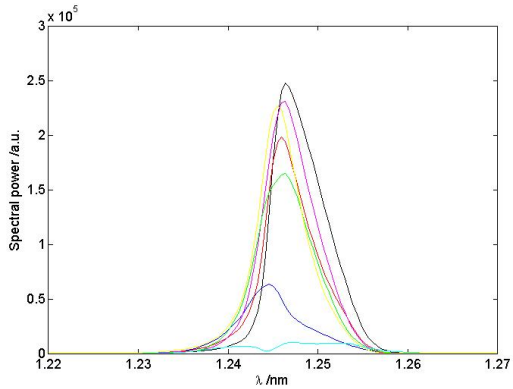

Figure 9: Example of the spectral profile for 7 pulses with different initial shot noise seeds.

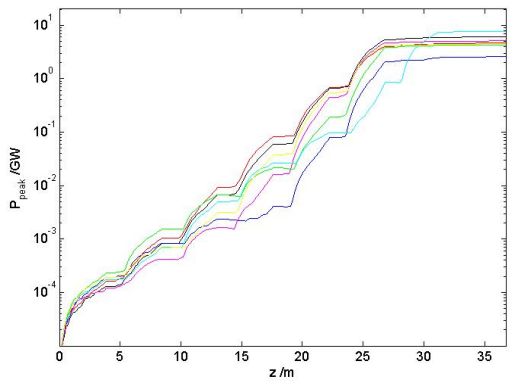

Figure 10: Peak power as a function of distance for the pulses shown in Figs. 8 and 9, highlighting the different saturation points within the undulator train.

Table 4: Intrinsic jitter in FEL ouput (no linac jitter).

	Mean	Relative rms
Peak power	3.2 GW	48%
Δt_{FWHM}	0.40 fs	19%
Spectral FWHM	0.0066 nm	22.1%
Peak Wavelength	1.25 nm	0.10%
Time-bandwidth	0.50	21.7%

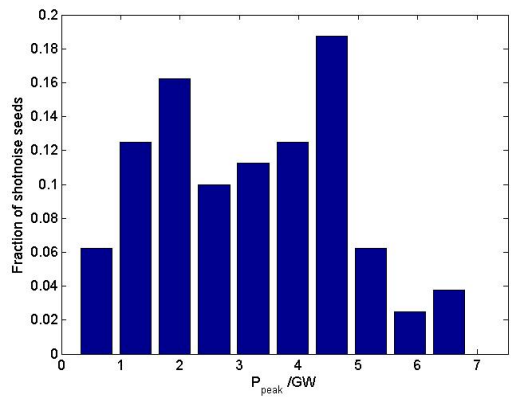

Figure 11: Histogram showing the variation in peak power over the 100 shot noise error seeds.

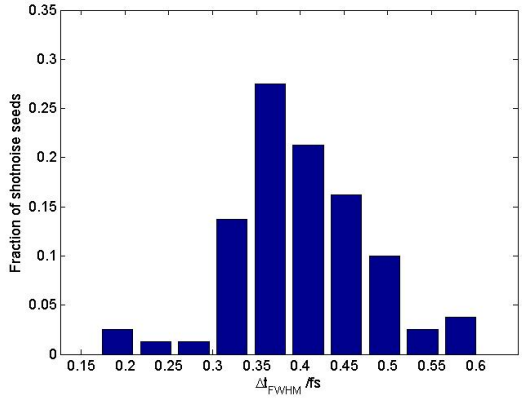

Figure 12: Histogram showing the variation in pulse width over the 100 shot noise error seeds.

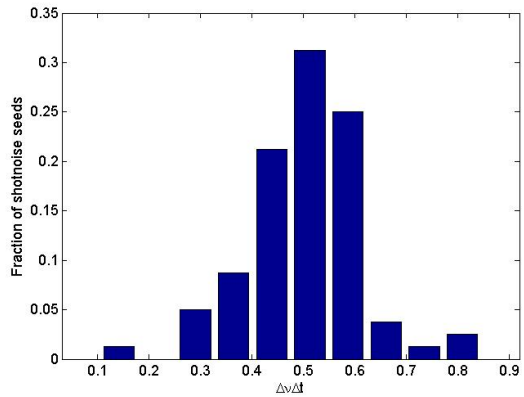

Figure 13: Histogram showing the variation in time-bandwidth product over the 100 shot noise error seeds.

CONCLUSIONS

We have analysed the possibility of operating the NLS FEL in single spike mode for the production of sub-fs 1 keV radiation pulses. The results show that a bunch charge of 2 pC is sufficient to produce single spike pulses with very interesting power levels. The analysis of the jitter effects show that time arrival jitter can be a potential limiting factor in the applicability of this type of FEL pulses. Tighter RF tolerances need to be considered.

We would like to acknowledge the contribution of T. Williams in carrying out the FEL jitter studies.

REFERENCES

[1] R.P. Walker et al., PAC'09, TU5RFP022; see also http://www.newlightsource.org/.
[2] R. Bonifacio et al., PRL, **73**, 70, (1994).
[3] S. Reiche et al., NIM **A593**, 45, (2008).
[4] M. Boscolo et al., NIM **A593**, 137, (2008).
[5] R. Bartolini et al., these proceedings.
[6] J.H. Han et al., to appear in PAC09 proceedings.
[7] K. Floettmann, www.desy.de/~mpyflo
[8] M. Borland, Advanced Photon Source, LS-287